Available online at www.sciencedirect.com
SCIENCE DIRECT®
Physics Letters A 344 (2005) 457–462
PHYSICS LETTERS A
www.elsevier.com/locate/pla

Exciton and biexciton binding and vertical Stark effect in a model lens-shaped quantum box: Application to InAs/InP quantum dots

C. Cornet *, J. Even, S. Loualiche

FOTON-UMR 6082 au CNRS, INSA de Rennes, 20 Avenue des Buttes de Coesmes, CS 14315, F-34043 Rennes Cedex, France

Received 16 May 2005; accepted 24 May 2005

Available online 5 July 2005

Communicated by V.M. Agranovich

Abstract

The problem of excitonic and biexcitonic binding is studied in the system of parabolic coordinates for a lens-shaped quantum box. The exciton wavefunction is expanded in terms of electron–hole configurations made from electron and hole single-particle states. Configuration interaction method and perturbative calculations are used to study the competition between confinement and correlation effects. Biexcitonic binding energy is calculated in the strong confinement regime and a comparison to the case of a spherical box is made. Absorption spectra with and without correlation effects are computed for InAs/InP quantum dots. Excitonic binding energy and enhancement factor are estimated to be equal to about 20 meV and 1.5, respectively. The excitonic absorption is finally studied in the presence of a uniform vertical electric field. A weak vertical Stark effect is predicted for lens-shaped quantum box described within this model.

PACS: 71.35.-y; 73.21.La

Keywords: Excitons and related phenomena; Quantum dots

1. Introduction

Recent research developments were devoted to nano-structured semiconductor materials. Quantum dots (QDs) may improve properties as compared to semiconductor quantum wells (QWs) for high performance optoelectronic devices [1–4]. Most of the theoretically predicted properties of the QDs have been experimentally demonstrated in the InAs/GaAs system [5–7]. In order to reach 1.55 μm wavelength used in optical telecommunications, growth of InAs QDs on InP substrate has been investigated in our laboratory [8–10]. Using simple one-band effective mass models, we have succeeded in obtaining a first description of the electronic properties of these QDs [11]. More accurate theoretical study of the electronic properties of QDs may be performed with various theo-

* Corresponding author.
E-mail addresses: charles.cornet@ens.insa-rennes.fr (C. Cornet), jacky.even@insa-rennes.fr (J. Even).

0375-9601/$ – see front matter
doi:10.1016/j.physleta.2005.05.103

retical schemes providing that precise descriptions of the size, shape and composition are given as input [12–14]. In the case of InAs/InP QDs however, data from characterization experiments are scarce. In such a case effective mass calculations for highly symmetric shapes (two-dimensional boxes [15], spherical QDs [2,16], ellipsoidal QDs [17]) may give indications about the influence of quantum confinement and correlation effects. These approaches are based on the fact that analytical expressions are known for the single-particle states wavefunctions. We recently proposed to use parabolic coordinates to obtain analytical solutions for the single-particle states in perfectly asymmetric lens-shaped QDs [18]. This work was extended to describe quantum wires and quantum rings within the same formalism [19]. In this work, we will focus on the calculation of excitonic and biexcitonic binding in lens-shaped QDs. The single-particle analytical wavefunctions will be used both for a perturbative approach and the configuration interaction (CI) method. The linear absorption spectra for InAs/InP QDs with and without Coulomb interaction will be compared. Finally, the excitonic absorption will be studied in the presence of a uniform vertical electric field.

2. Single-particle states

In the presence of an infinite potential barrier, the Schrödinger equation is equivalent to the Helmholtz equation [18]. The parabolic set of coordinate sets may be used to reach separable solutions described in Helmholtz equations. The parabolic set of unitless coordinates (u, v, ϑ) is defined by a transformation of Cartesian coordinates ($0 \leqslant u \leqslant \infty$, $0 \leqslant v \leqslant \infty$ and $0 \leqslant \theta \leqslant 2\pi$): $x = auv\cos(\vartheta)$, $y = auv\sin(\vartheta)$ and $z = a(u^2 - v^2)/2$ (a is the parameter of the parabolic metric). Then, for an infinite potential barrier the Hamiltonian is

$$\begin{aligned} H &= \frac{-\hbar^2}{2}\vec{\nabla}\frac{1}{m(\vec{r})}\vec{\nabla} \\ &= -\frac{\hbar^2}{2a^2(u^2+v^2)} \\ &\quad\times\left[\frac{1}{u}\frac{\partial}{\partial u}\frac{u}{m_{(u,v)}}\frac{\partial}{\partial u} + \frac{1}{v}\frac{\partial}{\partial v}\frac{v}{m_{(u,v)}}\frac{\partial}{\partial v}\right] \\ &\quad - \frac{\hbar^2}{2a^2u^2v^2m_{(u,v)}}\frac{\partial^2}{\partial\theta^2}. \end{aligned}$$

In that case, the Hamiltonian is separable in u, v and ϑ coordinates and the single-particle wavefunction appears a product of functions of independent variables $\Xi(u, v, \theta) = f(u)g(v)e^{in\theta}$. The f and g functions are solutions of two coupled differential equations with a separation constant C

$$u^2\frac{d^2f}{du^2} + u\frac{df}{du} + \left(Eu^4 - Cu^2 - n^2\right)f = 0$$

and

$$v^2\frac{d^2g}{dv^2} + v\frac{dg}{dv} + \left(Ev^4 + Cv^2 - n^2\right)g = 0,$$

where $E = E_r/E_{\infty P}$ a dimensionless energy, E_r the actual energy and $E_{\infty P} = \frac{\hbar^2}{2ma^2}$ a unit energy adapted to the parabolic system of coordinates. Solutions of these equations [18], include confluent hypergeometric functions of first kind ϕ

$$\begin{aligned} f(u) &= F(u, C, E, n) \\ &= \lambda_f e^{-i\sqrt{E}u^2/2}\left(i\sqrt{E}\,u^2\right)^{n/2} \\ &\quad\times\phi\left(\frac{-iC}{4\sqrt{E}} + \frac{n+1}{2}, n+1, i\sqrt{E}u^2\right) \end{aligned}$$

and

$$g(v) = F(v, -C, E, n) \quad (\lambda_f \text{ is a constant}).$$

A symmetric disk shape may be defined by the intersections of the two parabolas ($u = u_0 = 1$ and $v = v_0 = 1$) and rotated around the z axis (Fig. 1a). The height to diameter ratio (HDR) and volume V are equal respectively to 0.5 and $V = \pi a^3/2$. A relation between E and C is defined by the boundary conditions: $F(1, C, E, n) = 0$ [18]. If $C = 0$, the solutions of the problem contain simple $J_{n/2}(\sqrt{E}\,u^2/2)$ Bessel functions. This is in particular the case for the $1S$ ground state with $n = 0$ and $E = 23.1$. The solutions with $C \neq 0$ are twice degenerated: $\chi(u, v) = F(u, C, E, 0)^*F(v, -C, E, 0)$ and $\chi(u, v) = F(u, -C, E, 0)^*F(v, C, E, 0)$ with $E = 62.0$ and $C = 13.5$ correspond to the $2S$ state. Single-particle electronic states of a quantum box with flat bases (lens shape with HDR = 0.25 and $V = \pi a^3/4$) are readily obtained by keeping only odd solutions of the symmetric disk case with $C \neq 0$ [18]: $\chi(u, v) = F(u, C, E, 0)^*F(v, -C, E, 0) - F(u, -C, E, 0)^*F(v, C, E, 0)$. The $1S$ ground state of the lens-shaped QD corresponds to the $2S_u$ state of the disk-shaped QD

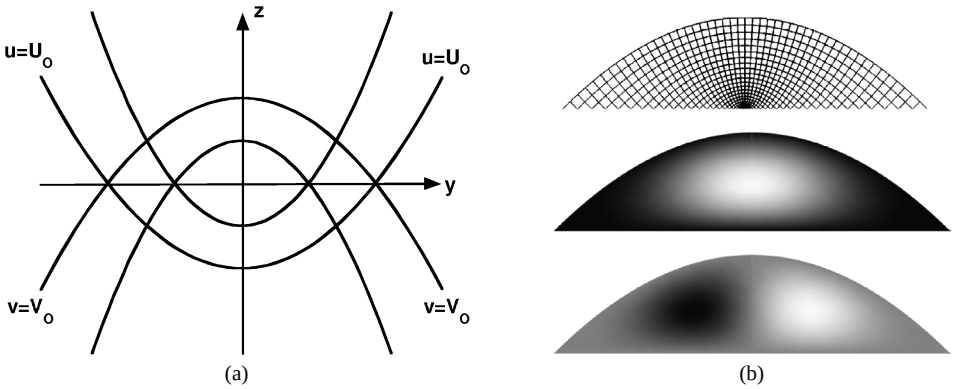

Fig. 1. (a) Projection of the parabolic coordinate surfaces in the (y, z) plane. A particular volume is obtained by the boundaries rotated around the z axis ($0 \leqslant \theta \leqslant 2\pi$). If two orthogonal confocal parabolas are used ($u_0 = 1$, $v_0 = 1$) a symmetrical disk-shaped box is obtained. (b) Cross section ((y, z) plane) of the parabolic mesh, the fundamental state $1S$ and first excited $1P$ wavefunctions for a lens-shaped quantum box with flat bases.

and the twice degenerated $1P$ excited states corresponds to the $1P_u$ states. The parabolic mesh and the probability density function for the $1S$ and $1P$ states are represented on Fig. 1b.

We may perform a first comparison for single-particle states energies between the spherical (sphere and hemisphere) and parabolic (disk and lens) system of coordinates. Using a common unit of energy $E_\infty = \frac{\hbar^2}{2mV^{2/3}}$ instead of $E_{\infty P} = \frac{\hbar^2}{2ma^2}$ and $E_{\infty S} = \frac{\hbar^2}{2mR^2}$, the ground state energy is then equal to 25.6, 33.1, 31.3 and 52.8 for a sphere, an hemisphere, a disk and a lens, respectively. The energy differences between the first excited state and the ground state are, respectively, equal to 26.8, 21.3, 22.2 and 21.8. It shows that the QD volume is the most important parameter but that symmetry properties and shape must be taken into account.

3. Excitonic binding

In order to study the excitonic and biexcitonic binding in lens-shaped QD, we follow the method used for spherical QDs [2,16]. The metric parameter plays the role of the radius R in spherical QDs. The dimensionless parameter $\lambda = \frac{a}{a_B}$, where a_B is the Bohr radius, is used for the calculations of the excitonic and biexcitonic energies ($\lambda = \frac{R}{a_B}$ in spherical QDs). The CI method and the perturbative approaches include the evaluation of the same interaction matrix elements: $U_{\alpha\beta} = \langle 0, 0|U|\alpha, \beta\rangle$ where $|0, 0\rangle$ is the uncorrelated electron–hole $|1S, 1S\rangle$ ground state, $|\alpha, \beta\rangle$ another pair state of the basis and $U = \frac{\lambda}{2}V(\vec{r}_e, \vec{r}_h)$ a renormalized electrostatic potential [2,16]. Notice that we neglect the dielectric mismatch between the QD and the barrier. We use also symmetry properties of the lens-shaped QD to evaluate the interaction matrix elements. In our previous work [18] the single-particle wavefunctions were classified according to the irreducible representation of the $C_{\infty v}$ symmetry group, with the quantum number n associated to the labels $S(n = 0), P(n = 1), D(n = 2), \ldots$. The Hamiltonian including the electron–hole interaction is invariant with respect to simultaneous rotation of the electron and hole around the z axis. $U_{\alpha\beta}$ matrix elements are then taken into account only for $|\alpha, \beta\rangle$ electron–hole pair states with $N = 0$ ($N = n_e + n_h$ is the total orbital angular momentum quantum number).

In the strong confinement regime ($\lambda \ll 1$), the excitonic binding energy is calculated from a first order perturbation including only the U_{00} matrix element. The excitonic binding energy is then equal to $-3.25\frac{e^2}{4\pi\varepsilon V^{1/3}}$ within this approximation for a lens-shaped quantum box. It can be compared to $-2.99\frac{e^2}{4\pi\varepsilon V^{1/3}}$ for the disk and $-2.89\frac{e^2}{4\pi\varepsilon V^{1/3}}$ for a sphere [2]. These results show that the dominant effect is associated to the volume. Shape plays the role of a secondary parameter if the anisotropy is not large as shown in Ref. [17]. In order to study the competition between confinement and correlation effects, it is necessary to go beyond the first order approximation. We choose material parameters relevant for InAs/InP QDs [11]. The relative dielectric constant is equal to

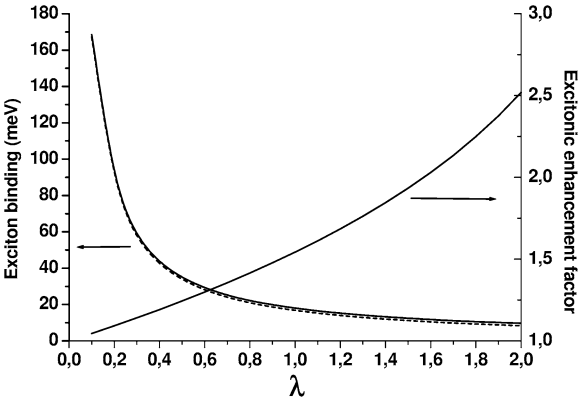

Fig. 2. Exciton binding energy (left vertical scale) calculated by first order perturbation (dotted line) and CI method as a function of λ. The excitonic enhancement factor is also reported as a function of λ (right scale).

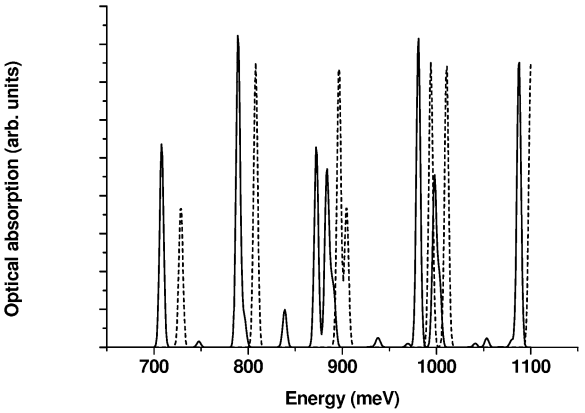

Fig. 3. Optical absorption calculated with (straight line) and without (dashed line) Coulomb effect. The lens-shaped InAs/InP QD corresponds to ($\lambda \sim 0.875$).

15.15, the electronic gap to 536 meV and the electron and hole effective masses to 0.05 and 0.2, respectively. The Bohr radius a_B is then equal to 20.0 nm and the Rydberg energy E_{Ryd} to 2.38 meV. Fig. 2 is a representation of the ground state exciton binding energy as a function of λ. The results of the first order perturbation and CI method are compared. The dotted line represents the results of the first order perturbation method with $-3.25\frac{e^2}{4\pi\varepsilon V^{1/3}} = -7.04\frac{E_{\mathrm{Ryd}}}{\lambda}$. It has been demonstrated in the litterature [20,21] that for small values of λ the binding energy of the exciton should decrease when λ decreases. This effect cannot be taken into account in our study because it is associated to finite potential barrier height and to the penetration of the wavefunction into the barrier. From our results, we deduce that for InAs/InP QDs with $a = 17.5$ nm [11], the excitonic binding energy is equal to 20.3 meV. For these QDs, the confinement regime is intermediate ($\lambda \sim 0.875$) and it is necessary to go a little bit beyond the first order approximation. We may notice that the excitonic binding energy is larger than the one ($4E_{\mathrm{Ryd}} = 9.5$ meV) of a QW with infinite potential barrier. On Fig. 2, the evolution of the excitonic enhancement factor is reported as a function of λ. This factor is the ratio of the ground state optical absorptions calculated with and without correlation effects. For InAs/InP QDs with $a = 17.5$ nm, this factor is equal to 1.5.

Fig. 3 is a comparison between the absorption spectra predicted for InAs/InP QDs ($a = 17.5$ nm) with and without correlation effects. The peaks have been convoluted by Gaussian functions in order to take into account the experimental broadening effect. The full width at half maximum of these functions is equal to 5 meV. The Coulomb interaction leads to a red-energy shift of the whole absorption spectrum by about one exciton binding energy. The effect of the excitonic enhancement factor is clearly visible when comparing both absorption spectra. We may also add that symmetry forbidden single-particle optical transitions become weakly allowed when the Coulomb interaction is taken into account.

In the strong confinement regime ($\lambda \ll 1$), the molecular biexcitonic binding energy E_{mol} is calculated from a summation of second order perturbation terms [2,15,16]. It is defined as the difference between the energy of a biexciton and the energy of two independent excitons. For InAs/InP QDs, the biexcitonic binding energy E_{mol} is equal to 3.6 meV. A general expression for a lower bound for this energy has been calculated for a spherical QD: $E_{\mathrm{mol}} > C(2 + \frac{m_e+m_h}{\mu})E_{\mathrm{Ryd}}$ where C is a constant equal to 0.052 [2, 16]. We have obtained the same expression for a lens-shaped quantum box with $C = 0.186$.

4. Stark effect

Electroabsorption effects near the band edge were studied in QW for applications like electroabsorption modulators or self-electrooptic effect devices [22]. It

may be interesting to evaluate how the stronger electronic confinement in QD when compared to QW may enhance the performances of such devices. First we may notice that the vertical Stark effect does not break the symmetry of the single-particle states contrary to the case of a model QW with an infinite potential barrier [22]. Linear Stark energy shifts $+0.228eFa$ and $+0.210eFa$ are calculated by first order perturbation for the $1S$ electronic ground state and the first excited $1P$ electronic state (F is a positive electric field oriented along the z axis). A variation of the intraband optical transition energy equal to $0.018eFa$ should then be observed. For InAs/InP QDs ($a = 17.5$ nm), it leads to a small variation of 3.2 meV for an electric field equal to 100 kV/cm. A quadratic Stark shift for the optical ground state transition is predicted because single-particle electron and hole wavefunctions are equivalent. There is no permanent dipole in the quantum box within this model. Second order perturbation term for the single-particle ground state in a QW is given by the expression $\Delta E = C(\frac{me^2F^2L^4}{\hbar^2})$ with $C = -2.2 \times 10^{-3}$ (L is the thickness of the QW and m is the effective mass of the electron or the hole). Using a similar expression for a lens-shaped quantum box where $L = a/2$ is the height, C is found equal to -1.8×10^{-3}. The interplay of excitonic and vertical Stark effects may be estimated simply by adding new terms to the CI Hamiltonian. The diagonalization of the Hamiltonian is restricted to the subspace of electron–hole pair states with $N = 0$. Fig. 4 is a representation of the absorption spectra of InAs/InP QDs ($a = 17.5$ nm) for various values of the electric field. A quadratic red-shift of the main ground state and excited state optical transitions is observed together with a decrease of the oscillator strengths. This effect appears smaller than the one in quantum well in agreement with previous studies [23] because the height of a QD is usually smaller than the thickness of a QW. In addition, a weak optical transition (indicated by an arrow) is enhanced by the vertical electric field.

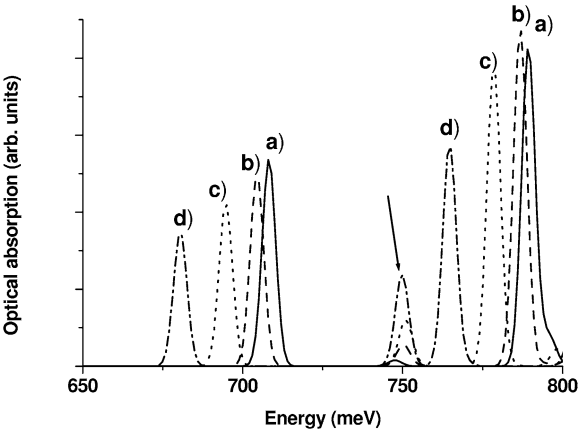

Fig. 4. Optical absorption calculated for various values of the external applied vertical electric field: (a) $E = 0$ kV/cm (straight line), (b) $E = 100$ kV/cm (dashed line), (c) $E = 200$ kV/cm (dotted line), (d) $E = 300$ kV/cm (dashed and dotted line). The lens-shaped InAs/InP QD corresponds to ($\lambda \sim 0.875$). A quadratic red-shift of the main optical ground state (left) and excited state (right) transitions is predicted. A weak optical transition (indicated by an arrow) is enhanced by the vertical electric field.

5. Conclusion

The problems of exciton and biexciton binding and vertical Stark effect in a lens-shaped quantum box were studied either with the CI method or with perturbative calculations using the analytical expressions of the single-particle wavefunctions [18]. In the strong confinement regime, the excitonic binding energy is given by an analytical expression with a volume dependence close to the one of a spherical quantum box. Excitonic and biexcitonic binding energies were estimated for InAs/InP QDs to be equal to 20.3 and 3.6 meV, respectively. The excitonic enhancement factor is found equal to 1.5. A linear Stark energy shift was calculated for the single-particle states but a quadratic effect is predicted for the optical ground state transition with an analytical expression similar to the one in QWs. As a result a weak vertical Stark effect is predicted for lens-shaped QDs described within this model.

References

[1] M. Grundmann, D. Bimberg, N.N. Ledentsov, Quantum Dot Heterostructures, Wiley, Chichester, 1998.
[2] L. Banyai, S.W. Koch, Semiconductor Quantum Dots, World Scientific Series on Atomic, Molecular and Optical Physics, vol. 2, World Scientific, Singapore, 1993.
[3] M. Sugawara, Self-Assembled InGaAs/GaAs Quantum Dots, Semiconductors and Semimetals, vol. 60, Academic Press, Toronto, 1999.

[4] Zh.I. Alferov, Quantum Wires and Dots Show the Way Forward III-Vs Rev. 11 (1998) 47.
[5] G.T. Liu, A. Stintz, H. Li, T.C. Newell, A.L. Gray, P.M. Varangis, K.J. Malloy, L.F. Lester, IEEE J. Quantum Electron. 36 (2000) 1272.
[6] H. Saito, K. Nishi, A. Kamei, S. Sugou, IEEE Photonics Technol. Lett. 12 (2000) 1298.
[7] O.B. Shcheckin, D.G. Deppe, IEEE Photonics Technol. Lett. 14 (2002) 1231.
[8] S. Frechengues, S. Bertru, N. Drouot, V. Lambert, B. Robinet, S. Loualiche, D. Lacombe, A. Ponchet, Appl. Phys. Lett. 74 (1999) 3356.
[9] C. Paranthoën, N. Bertru, B. Lambert, O. Dehaese, A. Le Corre, J. Even, S. Loualiche, F. Lissillour, G. Moreau, J.C. Simon, Semicond. Sci. Technol. 17 (2002) L5.
[10] C. Paranthoen, C. Platz, G. Moreau, N. Bertru, O. Dehaese, A. Le Corre, P. Miska, J. Even, H. Folliot, C. Labbe, G. Patriarche, J.C. Simon, S. Loualiche, J. Cryst. Growth. 251 (2003) 230.
[11] P. Miska, C. Paranthoen, J. Even, N. Bertru, A. Lecorre, O. Dehaese, J. Phys. Condens. Matter. 14 (2002) 12301.
[12] R. Heitz, O. Stier, I. Mukhametzhanov, A. Madhukar, D. Bimberg, Phys. Rev. B 62 (2000) 11017.
[13] C. Pryor, Phys. Rev. B 60 (1999) 2869.
[14] A. Zunger, Phys. Status Solidi (b) 224 (2001) 727.
[15] G.W. Bryant, Phys. Rev. B 41 (1990) 1243.
[16] L. Banyai, Phys. Rev. B 39 (1989) 8022.
[17] G. Cantele, D. Ninno, G. Iadonisi, Phys. Rev. B 64 (2001) 125325.
[18] J. Even, S. Loualiche, J. Phys. A: Math. Gen. 36 (2003) 11677.
[19] J. Even, S. Loualiche, J. Phys. A: Math. Gen. 37 (2004) L289.
[20] G.T. Einevoll, Phys. Rev. B 45 (1992) 3410.
[21] S. Le Goff, B. Stébé, Phys. Rev. B 47 (1993) 1383.
[22] S.L. Chuang, Physics of Optoelectronic Devices, in: Wiley Series in Pure and Applied Optics, Wiley, New York, 1995.
[23] S. Raymond, J.P. Reynolds, J.L. Merz, S. Fafard, Y. Feng, S. Charbonneau, Phys. Rev. B 58 (1998) R13415.